

1995

N95-70863

## MULTI-DIMENSIONAL COMBUSTOR FLOWFIELD ANALYSES IN GAS-GAS ROCKET ENGINE

Hsin-Hua Tsuei\* and Charles L. Merkle†  
Propulsion Engineering Research Center  
Department of Mechanical Engineering  
The Pennsylvania State University

### SUMMARY

The objectives of the present research are to improve design capabilities for low thrust rocket engines through understanding of the detailed mixing and combustion processes. Of particular interest is a small gaseous hydrogen-oxygen thruster which is considered as a coordinated part of a on-going experimental program at NASA LeRC. Detailed computational modeling requires the application of the full three-dimensional Navier Stokes equations, coupled with species diffusion equations. The numerical procedure is performed on both time-marching and time-accurate algorithms and using an LU approximate factorization in time, flux split upwinding differencing in space. The emphasis in this paper is focused on using numerical analysis to understand detailed combustor flowfields, including the shear layer dynamics created between fuel film cooling and the core gas in the vicinity on the nearby combustor wall; the integrity and effectiveness of the coolant film; three-dimensional fuel jets injection/mixing/combustion characteristics; and their impacts on global engine performance.

### TECHNICAL DISCUSSION

The first part of the current research stems from interest in the mixing layers that arise from film cooling in the combustor of a small chemical rocket engine [1-5]. This engine is a small gaseous hydrogen-oxygen engine originally designed to provide auxiliary propulsion and attitude control for Space Station Freedom. It provides about 110 N (25 lbf) of thrust and uses the entire hydrogen gas flow for regenerative cooling after which about two-thirds of it is split off for wall film cooling while the remaining one-third is mixed with the oxidizer and used for primary combustion. An unknown fraction of the hydrogen cooling film mixes with the oxidizer-rich core gas and burns between the injection plane and the throat. This combustion reduces the thickness of the coolant layer and weakens its effect, but also improves the overall efficiency of the thruster. The resulting shear region that is created between this coolant layer and the hot combustion gases in the core region takes on much of the character of a classical shear layer. This shear layer, however, incorporates not only a velocity difference, but also includes large molecular weight differences, chemical reactions and strong heat release. Classical shear layer instability, unsteady vortex roll-up and related shear layer dynamics can therefore be expected in the mixing layer. The vortex roll-up, however, will be confined by the presence of the adjacent wall and the subsequent roll-up will be diminished although the

---

\*Graduate Research Assistant

†Professor

unsteadiness remains. The issues of interest in the analysis are to document the role that these various mechanisms have on unsteady mixing in the shear layer and the integrity of the film of coolant adjacent to the wall.

Axisymmetric computational results have previously been compared with their experimental counterpart [3,4]. Comparisons have shown qualitative agreement, however, additional physics must be included to provide more accurate combustor flowfield predictions. Discrepancies arise mostly in the detailed local flowfield comparisons, including number density of major chemical species, the local temperature field and the exit velocity profile. In order to better understand where the disagreement stems from, an optical-access chamber was built in LeRC [3] to provide physical insight of the combustion chamber. Major chemical species and local temperature in the combustion chamber can therefore be detected by means of Raman scattering technique. Because the hydrogen fuel is injected through 12 ports around the chamber perimeter, detailed numerical modeling requires full three dimensional consideration to simulate the fuel jets and the mixing/ignition/combustion processes. The second part of this paper is thus centered on these issues. Preliminary three dimensional computational results for cold hydrogen fuel injection as well as the reacting flow calculations are presented. Efforts towards further comparisons with Raman measurement data are currently underway.

The numerical algorithm is based on extending earlier supersonic reacting flow calculations [6,7] to subsonic combustion problem [1,2,8]. The analysis uses an unsteady, three-dimensional, finite volume Navier-Stokes procedure that include chemical non-equilibrium effects. The governing equations can be written in a generalized coordinate system as :

$$\frac{\partial Q}{\partial t} + \frac{\partial}{\partial \xi}(E - E_v) + \frac{\partial}{\partial \eta}(F - F_v) + \frac{\partial}{\partial \zeta}(G - G_v) = H$$

where  $Q = (\rho, \rho u, \rho v, \rho w, e, \rho Y_i)^T$  is the vector of primary dependent variables, and  $E, F,$  and  $G$  are the inviscid flux vectors, and  $E_v, F_v,$  and  $G_v$  the viscous flux vectors in the  $\xi, \eta$  and  $\zeta$  directions, respectively. The vector  $H$  represents the source terms associated with chemical reactions or axisymmetry.

Numerical computation for steady flow is achieved by an implicit time-marching algorithm using an LU approximate factorization in time and flux split upwinding differencing in space. The time-accurate calculation for unsteady flow is conducted by a dual time stepping procedure [7]. The finite rate chemical reaction model used in the present work for gaseous hydrogen-oxygen combustion [6], involves nine chemical species and eighteen elementary reactions.

## RESULTS

To demonstrate the dynamics of unforced hydrogen-oxygen reacting shear layers in the gas-gas combustor, we begin by investigating the effects of the wall location. The upper wall is moved radially outward while the core gas passage and the width of the splitter plate remain unchanged. Figure 1 shows results of calculations for four different outer wall locations. The location of the splitter plate (radius of 10.3 mm) and the width of its base (1.3 mm) remain unchanged. The flow velocities are chosen to match the engine baseline operating condition: the hydrogen fuel (top portion) is injected at a speed of 125 m/s while the oxygen core flow (lower portion) enters at 185 m/s, giving a nominal velocity ratio of 0.67 and a density ratio of 16. The plots show contours of the OH concentration, a reasonable indicator of the instantaneous

diffusion flame location. In Fig. 1a, the outer wall is sufficiently far away from the shear layer (radius = 30 mm) that it has little effect on the vortex dynamics. The hydrogen-oxygen interface undergoes strong distortion and roll-up in the classical sense. The small bulge near the splitter plate represents the nucleus of the next succeeding roll-up. At an intermediate wall location (radius = 22 mm) some wall interaction is observed (Fig. 1b), but strong distortion is still present. The presence of the wall appears to cause the vortex to sweep forward more strongly than in Fig. 2a when the wall is further away. It is clear that the presence of the nearby wall affects the shape of the distorted shear layer. Figure 1c shows results for when the outer wall is brought still closer to the shear layer (radius = 17 mm). At this location the wall begins to prevent roll-up and diminish the unsteadiness. The distortion hits the outer wall before the entire roll-up process is completed, and the subsequent roll-up is forced to decay. Figure 1d shows results for the case when the outer wall is very close to the splitter plate (radius = 12.7 mm); the geometry of interest for the gas-gas combustor. A quick visual inspection shows the dominant influence of the adjacent wall. For this case, the wall is too close to the shear layer to allow the strong distortions seen in the previous two plots, and consequently the ensuing vortex roll-up does not occur. The shear layer does, however, maintain a substantial amount of unsteady oscillation. Performance computations [1-3] show that this unsteadiness causes a small decrease in the combustion rate of the fuel film with a corresponding decrease in performance.

In the engine combustor, hydrogen fuel used for primary combustion is injected radially through 12 annual ports, mixes with core oxygen then ignited by a spark plug. To accurately model the fuel jets mixing and combustion characteristics, three-dimensional consideration is required in the analyses. A cylindrical combustor without the spark plug is first used to demonstrate three-dimensional capability of the present theoretical model. Preheated core oxygen enters the combustor at 2000 K, 100 m/s while the hydrogen fuel is injected at 600 K, 600 m/s. For clarity, only one-quarter of the combustor, which contains three hydrogen injection ports, is plotted. The OH radical concentration contours and temperature contours are shown in Fig. 2a and 2b, respectively. In Fig. 2a, the dark contours represent higher OH radical concentration. It is observed that the shape of the diffusion flame is totally three-dimensional. The flame surface starts to wrinkle downstream of the hydrogen injectors because a recirculation region is formed behind each injection port that induces a vortex between the jet and the combustor wall. The hydrogen jets no longer maintain their near-cylindrical cross-sectional shape and deform in response to the vortical flow above them. The core oxygen gas therefore rolls up and wraps around each hydrogen jet causing further mixing and reaction near the combustor wall, resulting in a very high OH concentration region.

Figure 2b shows the temperature contours. Darkened contours indicate higher temperature, with a maximum temperature in the flame zone about 3600 K. It is also noted that the hydrogen jet is heated up due to heat transferred from the three-dimensional diffusion flame as it travels along the chamber.

To simulate the operating ignition condition, preliminary computation of cold hydrogen fuel injection into a cold oxygen core environment is investigated to provide perspective for the mixing processes under the designed operating condition. The spark plug is included in this calculation represented by the shaded region, located just upstream of the 12 hydrogen injection ports. A quarter of the combustor which involves three injection holes is again used to show the three-dimensional effects. The operating condition is chosen to match the experiment setup, with cold hydrogen injected at 325 m/s while the room temperature oxygen core enters at 13 m/s. Figure 3 shows the hydrogen mass fraction contours at two different time levels during the hydrogen injection process. Figure 3a shows an early stage shortly after the hydrogen injection is initiated. The mushroom-like mixing front is clearly observed. In Fig. 3b, after a certain amount of

hydrogen is pumped into the chamber, the mixture front keeps growing larger in size and turns toward the streamwise direction because of interactions with the core oxygen stream. A recirculation bubble is expected downstream of the spark plug, where the mixture is ignited. The computation is still currently underway while the ignition process will be initiated when a high enough mixture ratio is maintained in the recirculation region to sustain the flame after ignition. Further comparisons with experiment data will be made to validate the accuracy of the current analyses.

### ACKNOWLEDGEMENTS

This work has been supported by NASA Grant NAG 3-1020 and NAGW-1356. Partial computational support has been provided by the Center of Academic Computing at The Pennsylvania State University and the NAS Program at NASA Ames.

### REFERENCES

1. Tsuei, H.-H. and Merkle, C., AIAA Paper 94-0553, Reno, NV, 1994.
2. Tsuei, H.-H. and Merkle, C., Proc. 14th Intl. Conf. on Numerical Methods in Fluid Dynamics., Bangalore, India, 1994.
3. de Groot, W. and Tsuei, H.-H., AIAA Paper 94-0220, Reno, NV, 1994.
4. de Groot, W. and Weiss, J., AIAA Paper 92-3353, Nashville, TN, 1992.
5. Weiss, J. and Merkle, C., AIAA Paper 93-0237, Reno, NV, 1993.
6. Yu, S.-T., Tsai, Y.-L. P. and Shuen, J.-S., AIAA Paper 89-0391, Reno, NV, 1989.
7. Molvik, G. and Merkle, C., AIAA Paper 89-0199, Reno, NV, 1989.
8. Venkateswaran, S., Weiss, J., Merkle, C. and Choi, Y.-H., AIAA Paper 92-3437, Nashville, TN, 1992.

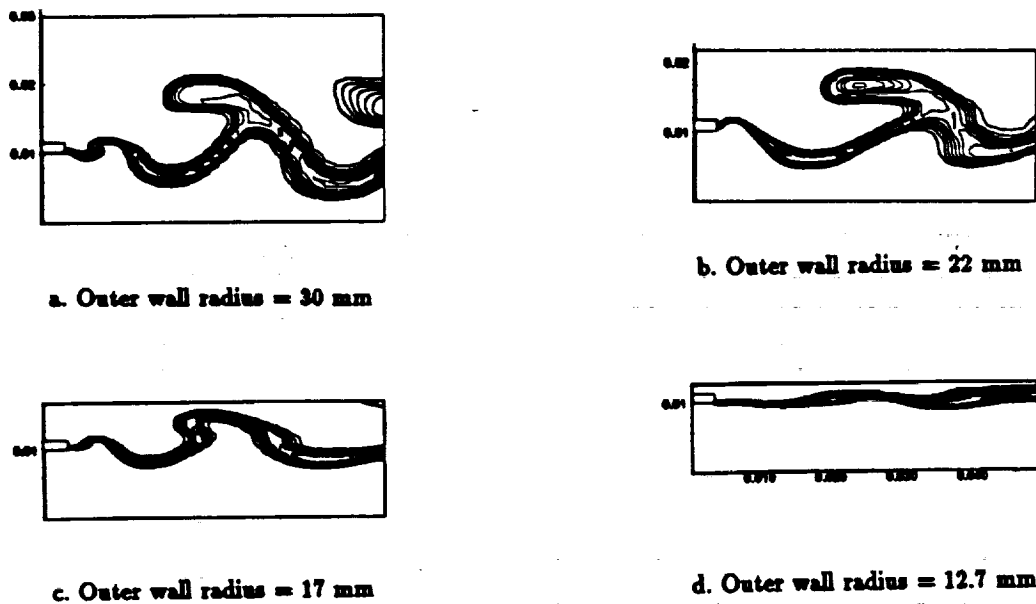


Figure 1. The OH radical concentration contours for four different outer wall locations.

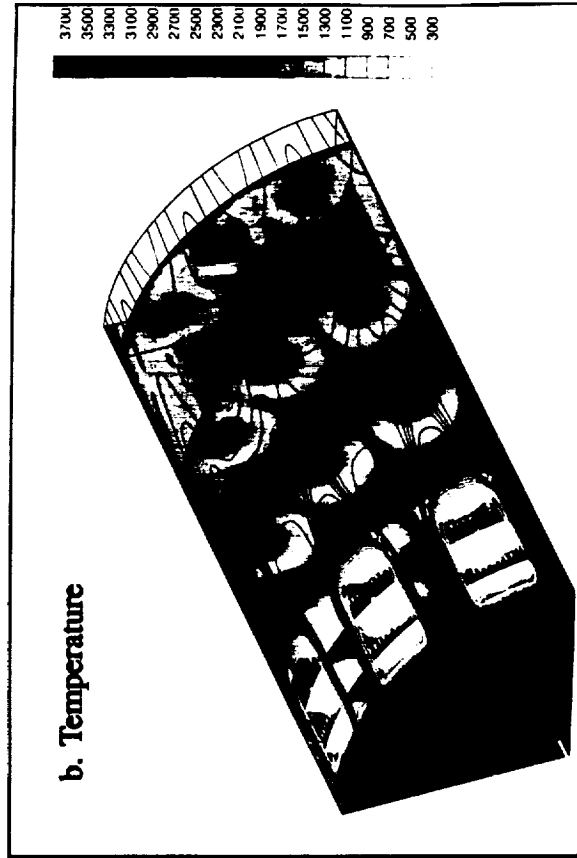
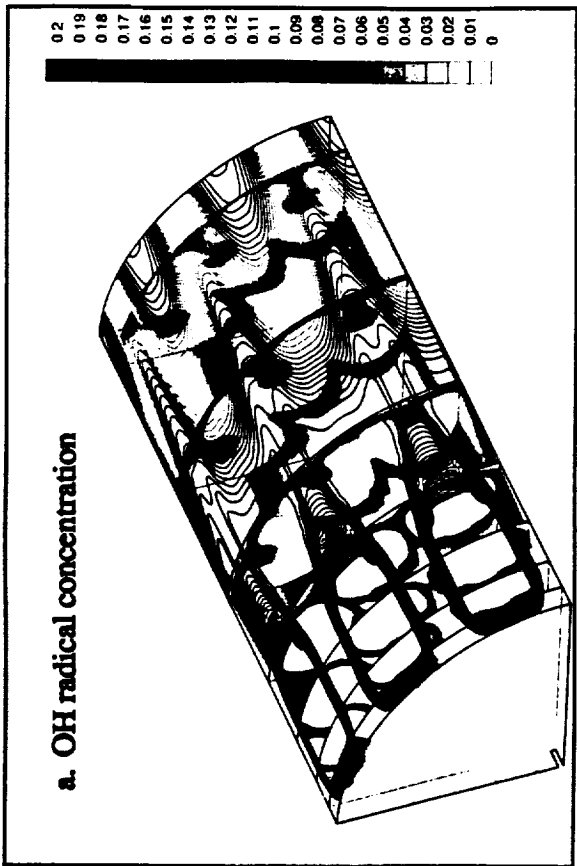


Figure 2. The OH radical concentration and temperature contours in one-quarter of the combustor.

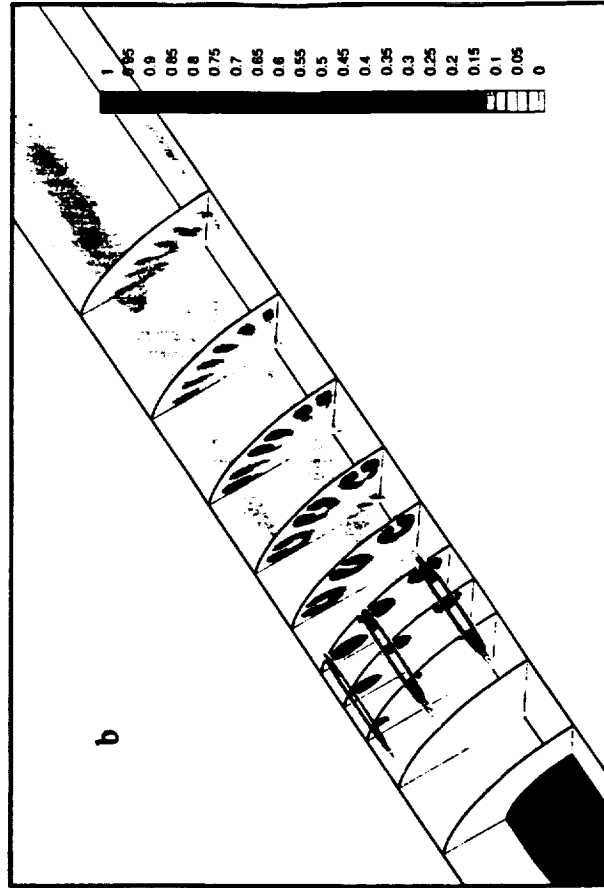
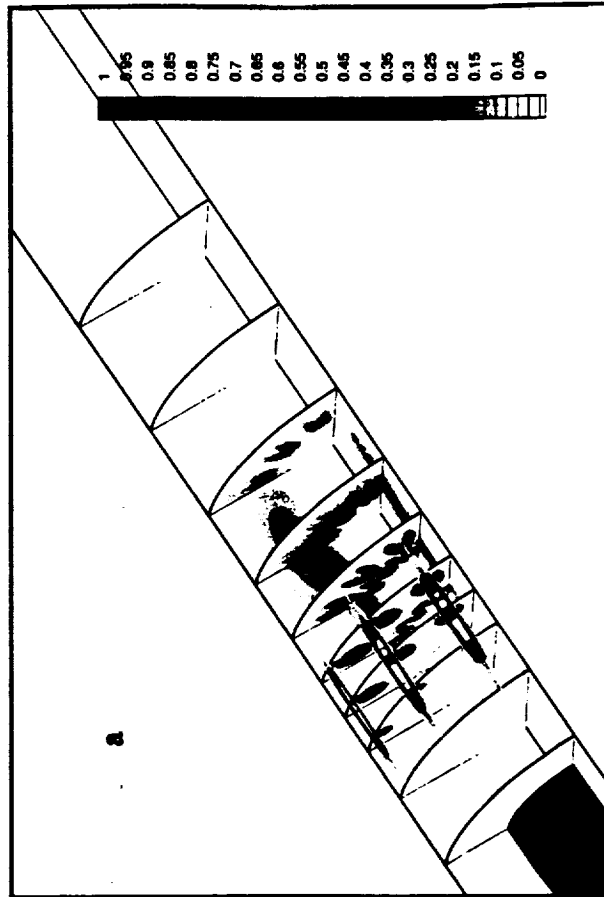


Figure 3. Hydrogen mass fraction contours at two different time levels during the injection process.